Modelling of soil bidirectional reflectance

Jerzy Cierniewski
Adam Mickiewicz University, Institute of Physical Geography and Environmental Planning, 61-701 Poznań, Poland

Tomasz Gdala
Student of Mathematical Methods of Computer Science, Poznań University of Technology, 60-965 Poznań, Poland

Assumptions to a geometrical model

A model, presented below, predicts the bidirectional reflectance of cultivated soil surfaces under any illumination and viewing conditions. It assumes that a rough soil surface *R* with a furrow micro-relief is spread on a *P* plane, simulating a soil slope oriented according to the horizontal plane *H* and the direction of the North *N* by the $_p$ and $_p$ angles, respectively. The azimuth angle $_c$ describes a direction of cultivation (Fig.1).

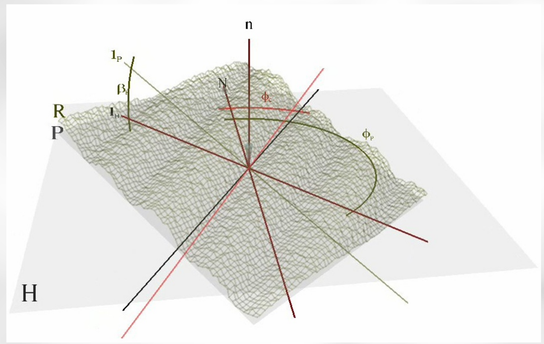

Fig. 1. Orientation of a simulated soil surface.

For simplification, the *R* surface consists of units iteratively duplicated. These units are constructed by a set of spheres of a given radius, suspended inside of a cube of dimension 1x1x1 (Fig.2). In a perpendicular projection, they are dispersed regularly in a net of squares. Their height is described by the *a* parameter describing the amplitude of the sinus function along *x*-axis, *b* expresses how strongly this amplitude is transfer along *y*-axis. Finally, the height of the sphere center is disturbed by the parameter *c*, which describes its maximum deviation in relation to values determined only by the *a* and *b* parameters. The *R* surface simulates a shape of a soil surface only if the spheres are deformed in that way that they remind drops merging themselves. This shape is recover from field reflectance data of an analyzed soil surface using a special procedure. First, many hundreds or thousands combinations of the *a*, *b* and *c* parameters are defined. Then, for each of these combinations, for the same illumination and viewing conditions as for the measured data, the reflectance distribution is generated by the model. All the generated data are compared with the measured data related to them, looking for those pare of these data, which gives the lowest root mean square error between the measured and the model generated data.

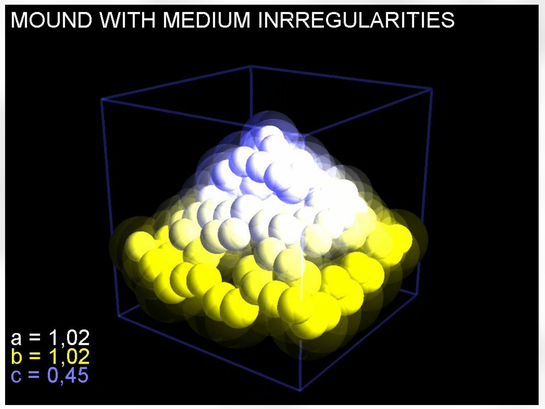

Fig. 2. Unit of a simulated soil surface.

A certain number of point sources evenly situated on the hemisphere, of a given intensity each, illuminates the *R* surface for a defined illumination conditions (Fig. 3). The position on the hemisphere where the intensity reaches the maximum on the hemisphere is described by the $_s$ and $_s$ angles.

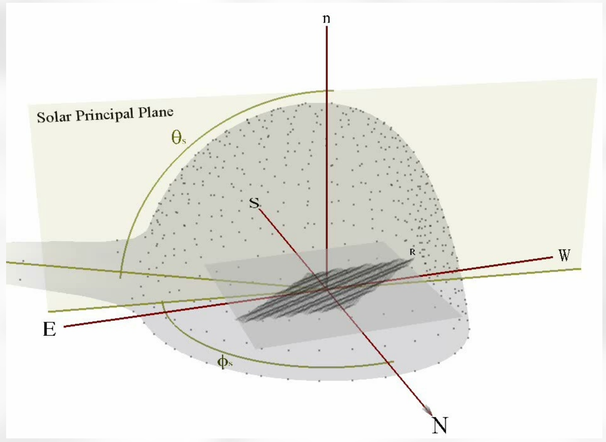

Fig. 3. Illumination of a soil surface.

Irregularities of the *R* surface can make impossible to illuminate the surface completely by all of the point sources on the hemisphere. The model assumes that energy coming from all unblocked point source to each fragment of the simulated surface is reflected in a specific way for a given soil material. Vectors of the energy leaving the elementary fragments create in the 3D space a specified cloud. Its shape and size change with variation of the incidence angle with respect to the normal to the fragment. This cloud describes the reflectance features of analyzed soil surface and is recovered from the measured reflectance data.

The *R* surface is viewed by a sensor, suspended over it, along a direction defined by the $_v$ and $_v$ angles (Fig. 4). The sensor, changing its position over the *R* surface, sums the length all of the vectors of the leaving energy along the direction $_v$, $_v$ from each elementary fragment of the surface *R* observed by the sensor as the effect of its illumination taken by each unblocked point light source on the hemisphere.

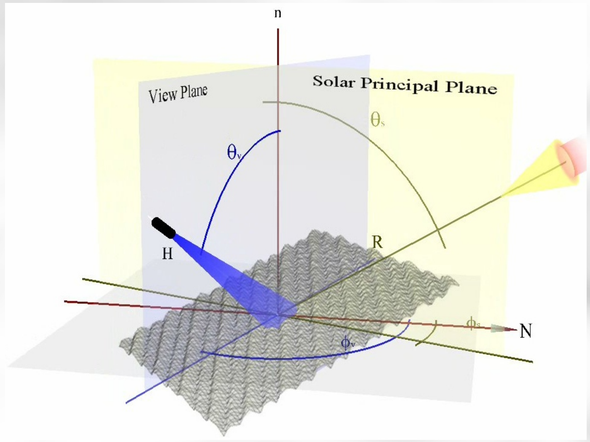

Fig. 4. Viewing of a soil surface by a sensor.

Examples of the model use

The model operation is presented on four examples of ploughed and harrowed surfaces, both as freshly prepared and after a few dozen mm rain (Fig. 5).

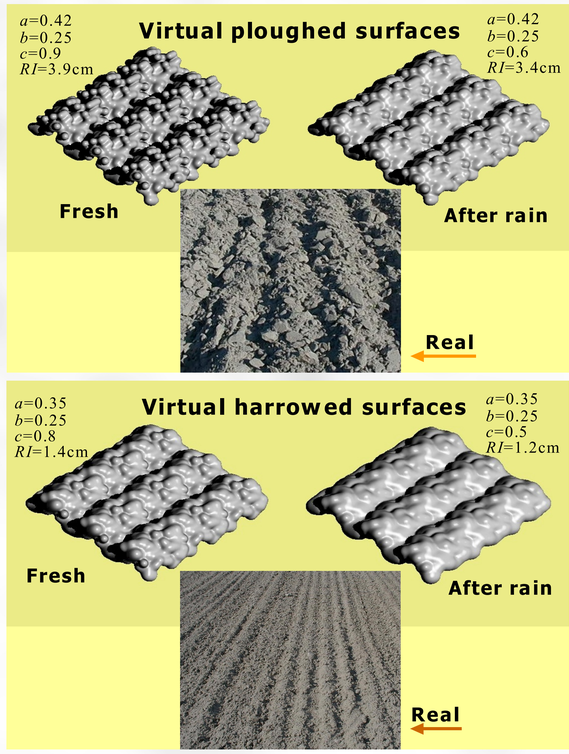

Fig. 5. Virtual surfaces with their geometry parameters (*a*, *b*, *c*), simulating reflectance behaviour of ploughed and harrowed surfaces as fresh and after rain, on the background of their real equivalents. The *RI* expresses their roughness index defined as the average deviation from their mean height.

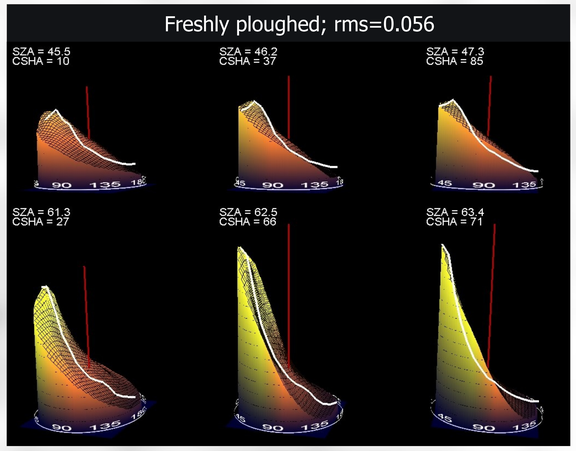

Fig. 6. Reflectance data of the freshly ploughed surface measured along the solar principal plane at different solar zenith angles (SZA) and the relative horizontal angles (CSHA) between the direction of cultivation and the direction of the sunbeams. They are drawn by white lines on the background of the data predicted by the model using the virtual surface also outside the solar principal plane. Fitting the predicted data to the measure ones characterize the average root mean square error *rms*.

rms *error between the measured and predicted reflectance of other surfaces*

Freshly ploughed	Ploughed, after rain	Freshly harrowed	Harrowed, after rain
0.056	0.048	0.061	0.052

Assuming that these virtual surfaces enough precisely (*rms*=0.48-0.61) (Fig. 6) enable us to predict the ploughed and harrowed soil bidirectional reflectance behaviour, we have analysed how its reflectance vary with changing the illumination of these surface furrows, expressed by the CSHA angle (Fig. 7). It is predicted for two solar zenith angles (SZA): 30° and 60°.

If the reflectance graphs, presented here, would be generated to help as to precise in which illumination and viewing conditions those ploughed and harrowed surfaces create maximum contrast to each other, and therefore their separation by remote sensing is easiest, we are be able to say that it is:

- for lower SZAs, than higher,
- for higher CSHA angle of furrow illumination than for lower, especially when the solar beams coming perpendicular to the direction of cultivation, and

when the surfaces are viewed by sensors from backscattering directions.

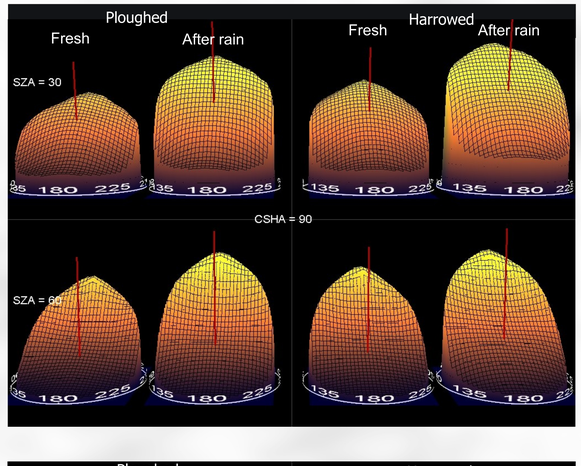

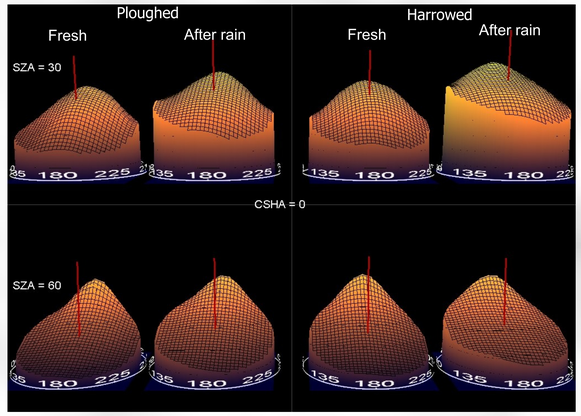

Fig. 7. Differences in the reflectance distribution between the ploughed and harrowed surfaces, both as fresh and after rain, generated by the model for 850 nm if their furrows are illuminated at the CSHA angles equals 0° and 90°.

Applications of the model

Thinking about other applications of those virtual surfaces together with the model presented here, we suppose they could be used as tools for:

- completing soil reflectance data at illumination and viewing conditions which are difficult for collection,
- accurate calculation of soil surface albedo from satellite level,

correction of satellite or aerial imageries of bare soil surfaces, eliminating effects of their non-Lambertian behavior, executed before final classification of those surfaces.